RSC Advances

PAPER

View Article Online
View Journal | View Issue

Cite this: *RSC Adv.*, 2016, **6**, 105573

Supramolecular activation of the photodynamic properties of porphyrinoid photosensitizers by calix[4]arene nanoassemblies†‡

Ivana Di Bari,[a] Aurore Fraix,[a] Roberta Picciotto,[a] Anna R. Blanco,[b] Salvatore Petralia,[c] Sabrina Conoci,[c] Giuseppe Granata,[d] Grazia M. L. Consoli*[d] and Salvatore Sortino*[a]

Received 21st September 2016
Accepted 31st October 2016

DOI: 10.1039/c6ra23492e

www.rsc.org/advances

Micellar-like nanocontainers *ca.* 40 nm in diameter of an amphiphilic calix[4]arene, encapsulate hydrophilic and hydrophobic phthalocyanine and porphyrin derivatives and effectively switch on their capability to photogenerate the cytotoxic singlet oxygen, otherwise totally precluded in water medium, with high quantum efficiency (Φ_Δ = 0.57 and 0.89). The photodynamic action of the supramolecular nanoassemblies is demonstrated by their remarkable inactivation under visible light irradiation of *Staphylococcus aureus* and *Pseudomonas aeruginosa*, representative Gram-positive and Gram-negative bacteria, respectively.

Introduction

In the search of novel antibacterial treatment modalities designed to face the problems of antibiotic Multi Drug Resistance (MDR)[1] and the low turnover of new clinically approved antibiotic drugs,[2] photodynamic therapy (PDT) constitutes a valid alternative against antibiotic-resistant bacteria.[3] This promising treatment modality takes advantage of the effects originated by the appropriate combination of visible light with a photosensitizer (PS) in the presence of molecular oxygen.[4] The excited PS transfers the energy of its lowest excited triplet state to nearby molecular oxygen, reverting to the ground state. This process results, in general, in the *in situ* production of singlet oxygen ($^1O_2$) which is accepted to be the foremost mediator of cytotoxic reactions in the cells.[5] $^1O_2$ offers important advantages over conventional antibiotic drugs as it: (i) potentially attacks biological substrates of different nature (*i.e.*, lipids, proteins, and DNA) representing a multitarget therapeutic agent, (ii) does not suffer MDR problems and (iii) due to their short half-life (<0.1 ms) and lack of charge, it diffuses in the cellular environment over short distances (few tens of nm) without inflicting systemic side effects.

Porphyrins and phthalocyanines play a central role as PSs in PDT by virtue of their high triplet quantum yields, very long triplet lifetimes, and strong absorption in the visible region, which are all key parameters for an effective photoproduction of $^1O_2$.[6] However, insolubility and/or aggregation of PSs in water medium represent the main drawbacks that limit their widespread application and that must be avoided in order to exploit the photosensitizing ability of these compounds.

Nanotechnology, offers good opportunities to overcome the above limitations by integration of PSs in a variety of organic, inorganic and hybrid nanomaterials.[7]

Calix[*n*]arenes are a family of polyphenolic macrocycles characterized by a remarkable synthetic versatility.[8] The opportune functionalization of the calixarene skeleton has provided amphiphilic derivatives able to assembly in a variety of well-defined supramolecular architectures suitable to entrap guests of different nature.[9] This feature associated to the low toxicity and immunogenicity exhibited by water soluble calixarenes,[10] has sponsored the calixarene-based assemblies for pharmaceutical applications.[11] Calixarene-based nanosystems for drug delivery have already been described.[12] However, applications of calixarenes as nanocarriers for PDT is rather limited and mainly focused to anticancer applications.[13]

Recently we have demonstrated that micellar aggregates of the amphiphilic calix[4]arene **1** (Fig. 1) effectively entrap a hydrophobic nitric oxide (NO) photoreleaser and act as nanoreactors that amplify the photogeneration of NO, resulting in a remarkable antibacterial activity against both Gram positive and Gram negative bacterial strains.[14]

In this paper, we demonstrate how this calixarene-based nanoassembly can also represent a versatile supramolecular host system for antimicrobial PDT applications. To this end, we have selected the two porphyrinoid PSs **2** and **3** as prototypes of hydrophilic and hydrophobic PSs (Fig. 1). Their choice is not casual but it is motivated by the fact that their photodynamic

[a]*Laboratory of Photochemistry, Department of Drug Science, Viale Andrea Doria 6, 95125, Catania, Italy. E-mail: ssortino@unict.it*

[b]*Clinical Development, SIFI S.p.A. Via Ercole Patti 36, Lavinaio, 95020 Catania, Italy*

[c]*STMicroelectronics, Stradale Primosole 50, 95121 Catania, Italy*

[d]*Institute of Biomolecular Chemistry, C.N.R., Via P. Gaifami, 18, I-95126, Catania, Italy. E-mail: grazia.consoli@icb.cnr.it*

† Dedicated to the memory of Carmela Spatafora.

‡ Electronic supplementary information (ESI) available: Absorption spectra, DLS and TEM. See DOI: 10.1039/c6ra23492e

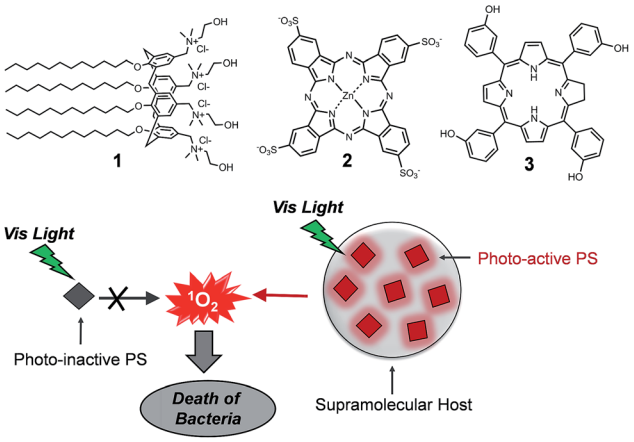

Fig. 1 Structures of the amphiphilic calix[4]arene **1** and the PS **2** and **3**.

properties are totally suppressed in water medium. In fact, the hydrophilic phthalocyanine **2** is well soluble in water solution but its complete aggregation precludes any response to light.[15] On the other hand, the hydrophobic porphyrin derivative **3** is photochemically inactive due to its complete insolubility in water medium. We demonstrate herein that the supramolecular entangling of the two prototype PSs within the micellar nanoassembly switches on their photodynamic properties with efficiency even higher than that observed in others cationic micelles or organic solvents. As a result, the supramolecular constructs exert effective bactericidal action against both *Staphylococcus aureus* and *Pseudomonas aeruginosa*, representative of Gram-positive and Gram-negative bacteria, respectively, in the absence of other growth attenuators.

Results and discussion

At concentration greater than 8 μM, the polycationic calixarene **1**, forms micellar-like supramolecular nanoaggregates with an average hydrodynamic diameter of *ca.* 40 nm, a polydispersity index < 0.2 and a zeta potential $\zeta = +24.7$ mV.[14] The hydrophilic phthalocyanine PS **2** is soluble in aqueous medium where it shows a single absorption band in the visible region at 600 nm ((a) in Fig. 2). According to literature, **2** is mostly self-aggregated and not photoresponsive under these conditions ((d) in Fig. 2).[15] However, in the presence of the calixarene **1** a remarkable amount of **2** (*ca.* 100%) can be entangled as monomeric species, as confirmed by the appearance of its typical absorption band at $\lambda_{max} = 680$ nm [15] ((b) in Fig. 2) accompanied by the disappearing of the absorption band of the aggregates and the revival of the characteristic red fluorescence ((e) in Fig. 2).[15]

According to its hydrophobic nature, the PS **3** is insoluble in aqueous medium and thus unable to act as effective PS. On the other hand, **3** can be entrapped in the nanoassemblies of **1** by a simple and reproducible protocol (see experimental) to give a colloidal solution in phosphate buffered saline solution at physiological pH, as confirmed by the appearance of the typical absorption spectrum covering the whole visible region ((a) in Fig. 3) and the characteristic red fluorescence emission ((c) in

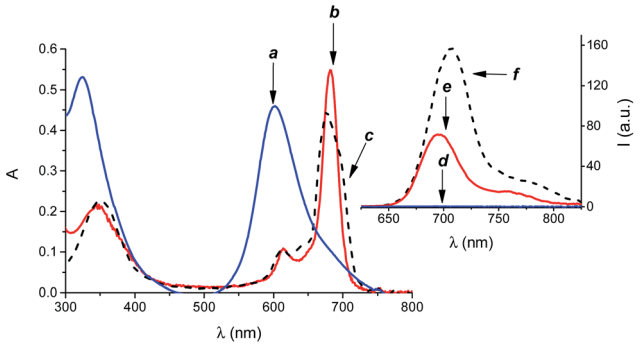

Fig. 2 Absorption spectra of **2** (15 μM) in phosphate buffered saline (pH 7.4, 10 mM) in the absence (a) and in the presence (b) of **1** (300 μM). Fluorescence emission spectra of **2** in phosphate buffered saline (pH 7.4, 10 mM) in the absence (d) and in the presence (e) of **1** (300 μM). The absorption (c) and fluorescence emission (f) spectra of **2** in DMSO, where it is present as monomeric species are also shown, for sake of comparison. $\lambda_{exc} = 540$ nm.

Fig. 3) of this PS, very similar to those observed in methanol solution ((b) and (d) in Fig. 3). The amount of **3** loaded was 3 μM, corresponding to an encapsulation efficiency of *ca.* 100%.

Interestingly, the encapsulation process did not change significantly the sizes of the calixarene-based micellar nanocontainer in a host : guest concentration range 100 : 1–100 : 25. Dynamic light scattering measurements gave hydrodynamic diameters of *ca.* 45 nm in both cases, suggesting a negligible rearrangement of the micellar aggregates upon loading of the PSs (Fig. S2 ESI‡), in a fairly good agreement with the Transmission Electron Microscopy Analysis (Fig. S3 ESI‡). On the other hand, a slight decrease of the zeta potential to a value $\zeta = +20.8$ mV was observed only in the case of the nanoassembly **1**·**2**, according to the anionic nature of the guest which partially compensates the cationic nature of the micellar host.

The supramolecular nanoassemblies were also investigated by Atomic Force Microscopy (AFM). Representative results for **1**·**2** are shown in Fig. 4 (similar results were obtained for **1**·**3**).

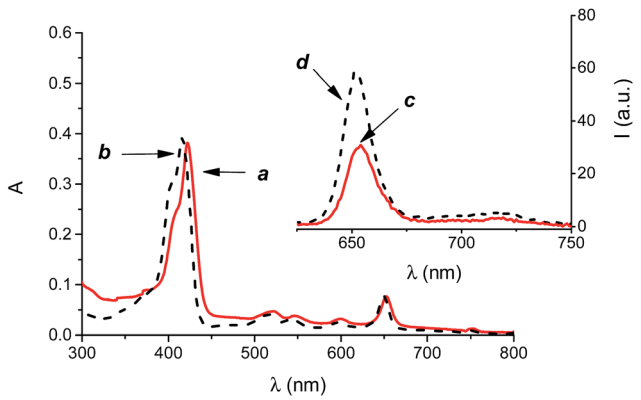

Fig. 3 Absorption (a) and fluorescence emission (c) spectra of **3** (3 μM) in phosphate buffered saline (pH 7.4, 10 mM) in the presence of **1** (300 μM). The absorption (b) and fluorescence emission (d) spectra of **3** in methanol are also shown, for sake of comparison. $\lambda_{exc} = 590$ nm.

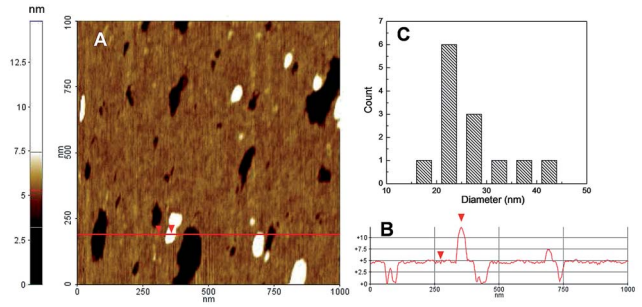

Fig. 4 (A) Contact mode AFM of the supramolecular nanoassembly **1·2** deposited on cleaned silicon surface. (B) Height line profile of line shown in (A). (C) Diameter distribution of the nanoassembly **1·2**.

Fig. 4A shows the two-dimension topography and the reports the height profile of continue red line shown in Fig. 4A. The AFM analysis gave a mean diameter of about 25 nm with a distribution in agreement with Poisson one within the range 16 and 44 nm (Fig. 4C). The difference in the diameter value observed with DLS technique could be mainly ascribed to the different environments in which the measurements are performed.[16]

Note that, the supramolecular construct **1·2** and **1·3** were stable for weeks under physiological conditions and their formation and stability are reasonably the result of both electrostatic and hydrophobic interactions between the amphiphilic host and the guests.

$^1O_2$ is the key species involved in the photodynamic action and the best experimental methodology to prove and quantify its production is its direct detection by its typical phosphorescence in the near-IR spectral window.[17] According to the massive aggregation of **2** and the insolubility of **3** in water medium, no $^1O_2$ signal was observed under these conditions. In contrast, the characteristic luminescence signals with maximum at *ca.* 1270 nm were observed for the supramolecular nanoassemblies **1·2** and **1·3** (Fig. 5). The quantum yield for $^1O_2$ photogeneration, Φ_Δ, were 0.57 and 0.89 respectively. These values are significantly higher than those observed for the **2** in CTAC micelles ($\Phi_\Delta = 0.31$)[18] and in DMSO ($\Phi_\Delta = 0.46$)[19] and for **3** in methanol ($\Phi_\Delta = 0.43$).[20] Note that, negligible photodegradation of the PSs was observed upon irradiation (see Fig. S1 ESI‡).

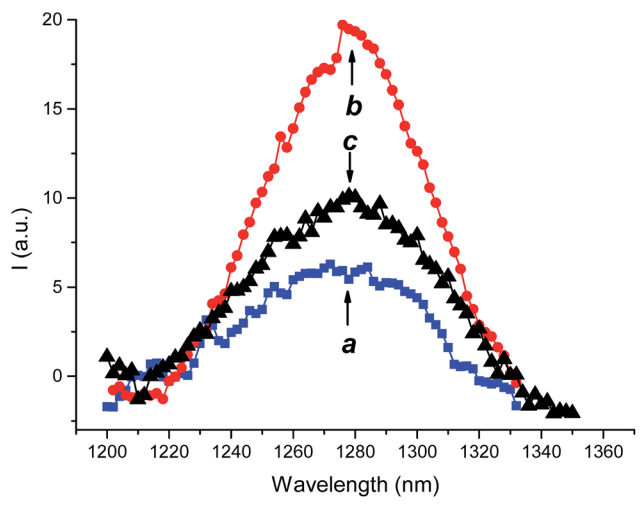

Fig. 5 $^1O_2$ luminescence detected upon excitation of the nanoassembly **1·2** at $\lambda_{exc} = 680$ nm (a) and the nanoassembly **1·3** at $\lambda_{exc} = 405$ nm (b) in deuterated phosphate buffered saline (pH 7.4, 10 mM). The $^1O_2$ luminescence spectrum observed for **3** in methanol is also shown, for sake of clarity (c).

The photodynamic properties of the supramolecular complexes were tested on *Staphylococcus aureus* ATCC 6538 and *Pseudomonas aeruginosa* ATCC 9027 specimens of Gram-positive and Gram-negative bacteria responsible for higher rate of morbidity due to the high antibiotic resistance pattern towards the traditional antibiotics. The bacterial cultures were kept in the dark or irradiated at different times with a 470 W xenon lamp equipped with a cut-off filter at 400 nm. The supramolecular nanoassemblies **1·2** and **1·3** did not show any significant antibacterial action in the dark. On the other hand, both the nanoassemblies induced significant inhibition upon irradiation in a fashion strictly dependent on the irradiation time (Fig. 6). In the case of **1·2** a complete growth inhibition of both bacteria strains was reached after only 10 min of illumination. Despite the Φ_Δ value for **1·2** was smaller than **1·3**, the shorter irradiation time required to observe the total inhibition of the

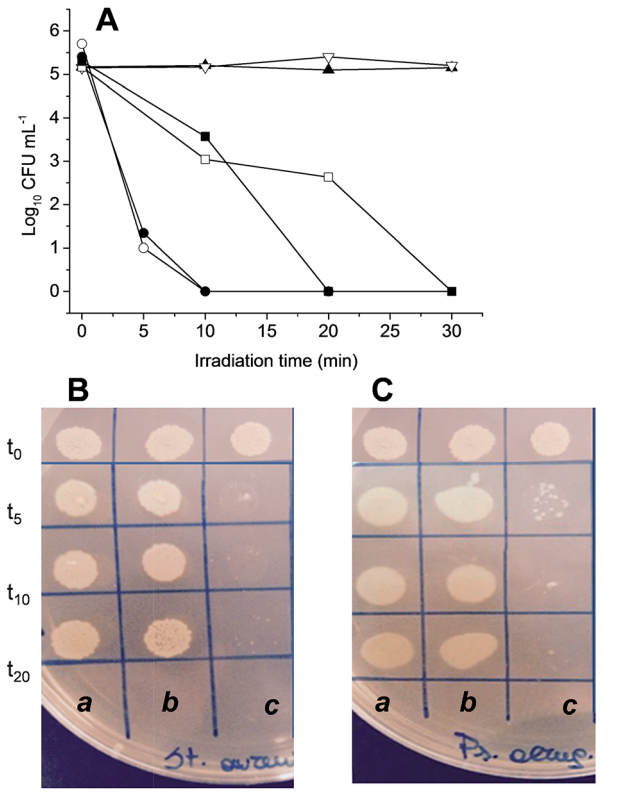

Fig. 6 (A) Time-kill curves of the nanoassembly **1·2** (circles), **1·3** (squares) and, for comparison, **1** alone (triangles) observed for *Staphylococcus aureus* ATCC 6538 (open symbols) and *Pseudomonas aeruginosa* ATCC 9027 (filled symbols). Representative images for the antibacterial effect observed on *Staphylococcus aureus* ATCC 6538 (B) and *Pseudomonas aeruginosa* ATCC 9027 (C) at different irradiation times of (a) control, (b) **1** and (c) **1·2**. [**1**] = 300 μM, [**2**] = 15 μM; [**3**] = 3 μM.

bacteria growth in this case may be the result of the large fraction of absorbed photons by this nanoassembly if compared with **1**·**3**.

Conclusions

We have demonstrated that a supramolecular nanoassembly of a calix[4]arene derivative represents a versatile supramolecular host to encapsulate prototypes of hydrophilic and hydrophobic porphyrinoid (PSs). Their effective entangling not only switch on their photodynamic properties, otherwise totally precluded in water medium, but also improves their quantum efficiency, if compared with other micellar systems and organic solvents. Effective bactericidal action is demonstrated against both Gram-negative and Gram-positive bacteria strains. To the best of our knowledge, these are the first examples where antibacterial PDT based on calixarene nanoassemblies is demonstrated. These finding, combined with small sizes and the good time stability in the dark, make the present nanoassemblies intriguing systems to be tested on a larger variety of bacterial colonies and to be co-loaded with the recently reported NO photogenerator.[14] At this regards, in view of the oxygen-independence of the NO photogenerators, nanoconstructs able to simultaneously photogenerate $^1O_2$ and NO may offer great potential in fighting both aerobic and anaerobic bacteria through bimodal action. These investigations are currently underway in our laboratories.

Experimental section

Materials

All reagents were of high commercial grade and were used without further purification. All solvents used were analytical grade. Calixarene **1** was synthesized according to the procedure described elsewhere.[14,21] The PS **2** and **3** were purchased from Porphyrin Pdts and Allorachem SRL, respectively and were used as received. *Staphylococcus aureus* (ATCC 6538) and *Pseudomonas aeruginosa* (ATCC 9027) were purchased from LGC Standards.

Preparation of the nanoassemblies

The supramolecular nanoassembly **1**·**2** was prepared by mixing the calixarene **1** (5 mg, 300 μM) and compound **2** (15 μM) in 10 mL of 10 mM phosphate buffered saline pH 7.4. The mixture was stirred for 15 days at room temperature and then filtered with 0.2 μm filter (GHP, Acrodisc) to remove any residual aggregate form. For the preparation of the nanoassembly **1**·**3**, compound **3** was firstly dissolved in methanol and slowly evaporated to form a thin film. The film was then hydrated with a phosphate buffered saline solutions of **1** (5 mg, 300 μM). The mixture was stirred for 10 days at room temperature and then filtered with 0.2 μm filter to remove any unentrapped compound **3**.

Instrumentations

^1H and ^{13}C NMR spectra were recorded on a Bruker Avance 400.13 and 100.13 MHz, respectively.

UV-Vis spectra absorption and fluorescence emission spectra were recorded with a JascoV-560 spectrophotometer and a Spex Fluorolog-2 (mod. F-111) spectrofluorimeter, respectively, in air-equilibrated solutions, using either quartz cells with a path length of 1 cm. $^1O_2$ emission was registered with the same spectrofluorimeter equipped with a NIR-sensitive liquid nitrogen cooled photomultiplier, exciting the air-equilibrated samples of the nanoassemblies **1**·**2** and **1**·**3** at 680 nm with the fluorimeter lamp or at 405 nm with a 200 mW continuum laser, respectively.

DLS measurements and zeta potential measurements were performed with a ZetaSizer NanoZS90 Malvern Instrument (UK), equipped with a 633 nm laser (scattering angle = 90°, T = 25 °C).

AFM images were acquired in air by using a Digital 3100 in tapping mode. Commercially available tapping etched silicon probes (Digital) with a pyramidal shape tip having a nominal curvature of 10 nm and a nominal internal angle of 35° were used. The samples for AFM analysis were prepared as follows: an aliquot (10 μL) of the nanoassembly solution was deposited on freshly cleaned silicon flat substrate (silicon substrate was cleaned by plasma-O_2 process for 10 min at 100 W). Afterwards, the residue liquid on the surface was removed. The sample was dried in air before the measurement.

Determination of the $^1O_2$ quantum yields

$^1O_2$ quantum yields were determined by using optically matched solution at the excitation wavelength of the nanoassemblies and the standard. Methylene blue in CH_2Cl_2 (Φ_Δ = 0.57)[22] and compound **3** in methanol (Φ_Δ = 0.43)[20] were used as a standard for **1**·**2** and **1**·**3**, respectively. The values of Φ_Δ for the nanoassemblies were determined by using the following equation:[23]

$$\Phi_\Delta = \Phi_{\Delta(s)}(In^2k_{r(s)}/I_{(s)}n_{(s)}{}^2k_r)$$

where $\Phi_{\Delta(s)}$ is the $^1O_2$ quantum yield of the standard, I and $I_{(s)}$ are the areas of the emission spectra of the nanoassembly and the standard, respectively; k_r and $k_{r(s)}$ are the $^1O_2$ radiative rate in the solvents used for the compound and standard; n and $n_{(s)}$ are the refraction index of the solvents used for the compound and the standard.

Antibacterial experiments

The day before performing the experiments, pure cultures were inoculated in 100 mL nutrient broth and incubated (37 °C, 24 h) to allow complete growth in the liquid growth medium. The overnight incubated broth culture was centrifuged at 4000 rpm for 15 minutes. Supernatant nutrient broth was discarded leaving bacterial pellet at the bottom of the centrifuge tube. PBS (5 mL) was added to the tube and the bacterial pellet was washed by shaking it gently. The washed pellet was again centrifuged at 2933 × g for 15 minutes. The pellet thus formed

was then diluted with PBS. For experiment, bacteria were inoculated in 96 well plate to yield a final inoculum of *ca.* 2–5 × 10^5 CFU mL^{-1}. Then calixarene **1** only and either **1**·**2** or **1**·**3** were added. Two different control samples were also prepared in PBS and Mueller Hinton. Before exposure to light, the samples to be irradiated were incubated in dark for 30 minutes. 15 μL of each sample was taken and seeded as a spot in a ground plate of Mueller Hinton supplemented with agar (time t_0). Irradiation was performed with a xenon lamp SUNTEST 470 W lamp mounting a cut-off filter at 400 nm. The light source was designed in such a way so as to fit over the 5 cm culture plate with a fixed distance of irradiation of 15 mm. The surface temperature of the samples was continuously recorded in order to avoid any significant rise in temperature. At different time, 15 μL of each sample was taken and seeded as a spot in a ground plate of Mueller Hinton supplemented with agar. The viability count for each sample was done in duplicate plates.

Acknowledgements

We thank the Marie Curie Program (FP7-PEOPLE-ITN-2013, CYCLON-HIT 608407) for financial support.

Notes and references

1 (*a*) G. Taubes, *Science*, 2008, **321**, 356; (*b*) M. L. Cohen, *Nature*, 2000, **406**, 762; (*c*) R. Laxminarayan, A. Duse, C. Wattal, A. K. Zaidi, H. F. Wertheim, *et al.*, *Lancet Infect. Dis.*, 2013, **13**, 1057.

2 D. M. Shlaes, D. Sahm, C. Opiela and B. Spellberg, *Antimicrob. Agents Chemother.*, 2013, **57**, 4605.

3 (*a*) M. R. Hamblin and T. Hasan, *Photochem. Photobiol. Sci.*, 2004, **3**, 436; (*b*) T. A. Maisch, *Mini-Rev. Med. Chem.*, 2009, **8**, 974; (*c*) M. A. Biel, in *Photodynamic Therapy: Methods and Protocol*, ed. G. J. Gomer, Springer, 2010, pp. 175–194.

4 (*a*) A. P. Castano, P. Mroz and M. R. Hamblin, *Nat. Rev. Cancer*, 2006, **6**, 535; (*b*) J. P. Celli, B. Q. Spring, I. Rizvi, C. L. Evans, K. S. Samkoe, S. Verma, B. W. Pogue and T. Hasan, *Chem. Rev.*, 2010, **12**, 2795.

5 (*a*) I. J. McDonald and T. J. Doughery, *J. Porphyrins Phthalocyanines*, 2001, **5**, 105; (*b*) T. Hasan, A. C. E. Moor and B. Ortel, *Cancer Medicine*, Decker BC Inc., Hamilton, Ontario, Canada, 5th edn, 2000.

6 (*a*) M. Wainmwright, *Photosensitizers in Biomedicine*, Wiley-Blackwell, 2009; (*b*) R. Pandey and G. Zheng, in *The Porphyrin Handbook*, ed. K. M. Smith, K. Kadish and R. Guilard, Academic Press, San Diego, 2000, vol. 6, pp. 157–230.

7 See, for example: (*a*) S. Wang, R. Gao, F. Zhou and M. Selke, *J. Mater. Chem.*, 2004, **14**, 487; (*b*) C. A. Strassert, M. Otter, R. Q. Albuquerque, A. Höne, Y. Vida, B. Maier and L. De Cola, *Angew. Chem., Int. Ed.*, 2009, **48**, 7928; (*c*) N. Nishiyama, A. Iriyama, W.-D. Jang, K. Miyata, K. Itaka, Y. Inoue, H. Takahashi, Y. Yanagi, H. Koyama and K. Kataoka, *Nat. Mater.*, 2005, **4**, 934.

8 For general reviews on calixarenes: (*a*) C. D. Gutsche, *Calixarene Revisited*, Royal Society of Chemistry, Cambridge, 1998; (*b*) Z. Asfari, V. Böhmer, J. Harrowfield and J. Vicens, *Calixarene*, Kluwer, Dordrecht, 2001; (*c*) J. Vicens and J. Harrowfield, *Calixarenes in the Nanoworld*, Springer, Dordrecht, 2007; (*d*) P. Neri, J. L. Sessler and M.-X. Wang, *Calixarenes and Beyond*, Springer, Berlin-Heidelberg, 2016.

9 (*a*) G. Granata, G. M. L. Consoli, R. Lo Nigro, G. Malandrino and C. Geraci, *Supramol. Chem.*, 2016, **28**, 377; (*b*) A. R. Blanco, M. L. Bondì, G. Cavallaro and G. M. L. Consoli, *et al.*, Patent WO2016055976A1, 2016; (*c*) G. M. L. Consoli, G. Granata and C. Geraci, *Org. Biomol. Chem.*, 2011, **9**, 6491; (*d*) G. M. L. Consoli, G. Granata, R. Lo Nigro, G. Malandrino and C. Geraci, *Langmuir*, 2008, **24**, 6194.

10 (*a*) P. Shahgaldian and A. W. Coleman, *Langmuir*, 2003, **19**, 5261; (*b*) M. H. Paclet, C. F. Rousseau, C. Yannick, F. Morel and A. W. Coleman, *J. Inclusion Phenom. Macrocyclic Chem.*, 2006, **55**, 353.

11 (*a*) C. Hoskins and A. D. M. Curtis, *Journal of Nanomedicine Research*, 2015, **2**, 00028; (*b*) M. D. Shah and Y. K. Agrawal, *J. Sci. Ind. Res.*, 2012, **71**, 21.

12 Y. Zhou, H. Li and Y.-W. Yang, *Chin. Chem. Lett.*, 2015, **26**, 825.

13 (*a*) Y. Cakmak, T. Nalbantoglu, T. Durgut and E. U. Akkaya, *Tetrahedron Lett.*, 2014, **55**, 538; (*b*) H. Yan, X. Pan, M. H. Chua, X. Wang, J. Song, Q. Ye, H. Zhou, A. T. Y. Xuan, Y. Liu and J. Xu, *RSC Adv.*, 2014, **4**, 10708; (*c*) C. Tu, L. Zhu, P. Li, Y. Chen, Y. Su, D. Yan, X. Zhu and G. Zhou, *Chem. Commun.*, 2011, **47**, 6063; (*d*) M. Neagu, R.-M. Ion, G. Manda, C. Constantin, E. Radu and Z. Cristu, *Rom. J. Biochem.*, 2010, **47**, 17.

14 I. Di Bari, R. Picciotto, G. Granata, A. R. Blanco, G. M. L. Consoli and S. Sortino, *Org. Biomol. Chem.*, 2016, **14**, 8047.

15 L. Howe and J. Z. Zhang, *J. Phys. Chem. A*, 1997, **101**, 3207.

16 F. Hoffmann, J. Cinatl, H. Kabicková, J. Kreuter and F. Stieneker, *Int. J. Pharm.*, 1997, **157**, 189.

17 F. Wilkinson, W. P. Helman and A. B. Ross, *J. Phys. Chem. Ref. Data*, 1993, **22**, 113.

18 W. Spiller, H. Kliesch, D. W. Herle, S. Hackbarth, B. R. Der and G. Schnurpfeil, *J. Porphyrins Phthalocyanines*, 1998, **2**, 145.

19 A. Ogunsipe, J.-Y. Chen and T. Nyokong, *New J. Chem.*, 2004, **28**, 822.

20 R. Bonnett, P. Charlesworth, B. D. Djelal, S. Foley, D. J. McGarvey and T. G. Truscott, *J. Chem. Soc., Perkin Trans. 2*, 1999, 325.

21 R. V. Rodik, A.-S. Anthony, V. I. Kalchenko, Y. Mely and A. S. Klymchenko, *New J. Chem.*, 2015, **39**, 1654.

22 L. Huang, X. Yu, W. Wu and J. Zhao, *Org. Lett.*, 2012, **14**, 2594.

23 A. P. Darmanyan, *J. Phys. Chem. A*, 1998, **102**, 9833.